GPS BASED LAND VEHICLE POSITIONING USING GAUSSIAN SUM FILTERS

A.Y. Kibangou and A. Monin

LAAS, CNRS, University of Toulouse, 7 av. colonel Roche, 31077 Toulouse Cedex, France

ABSTRACT

In this paper, we consider land vehicle positioning in an urban environment. A nonlinear and non-Gaussian model is derived as the process model whereas GPS pseudo-range and odometer measurements are used as observations. A parametric model is proposed for representing the variations of the observation noise covariance matrix. The performances of the derived Gaussian sum filter are evaluated by using experimental data.

***Index Terms*—** Global Positioning System, Land vehicles, Nonlinear filters, Jump processes

1. INTRODUCTION

Nowadays, the Global Positioning System (GPS) is extensively used as a navigation system due to its world-wide coverage, low cost, and accuracy. GPS receivers are commonly installed in vehicle as a key tool for providing new services to customers such as real-time traffic information, emergency calls, route guidance, fleet management, or advanced driving assistance systems [1].

Any vehicle equipped with a GPS receiver can determine its position in real time by measuring the time delays of signals from in-view satellites, hence range measurements. Typically, the range measurements, also called pseudo-ranges, are corrupted by receiver and satellites clock biases, ephemeris errors, ionospheric and tropospheric delays. These error sources can be reduced or eliminated by augmentation systems such as differential operation with geostationary satellites. That is the case of the European augmentation of GPS named EGNOS (European Geostationary Overlay Service).

However, there are many situations where a GPS solution is either unavailable or unreliable. The first case occurs when GPS signals do not reach the antenna due to shading effects resulting from high rise buildings and underpasses present in an urban environment. The second situation arises from poor satellite geometry and the multiple reflections of signals leading to multipath, which is a local phenomenon unsolvable by augmentation operations.

Multipath is certainly the major problem limiting the accuracy of a GPS solution in an urban environment. Several solutions have been proposed for mitigating the multipath effects. They are aimed either to recover the unbiased propagation delay or to compensate for the induced errors on GPS measurements. A wide range of techniques has been proposed in the first case. Some of these techniques require modifying the receiver architecture [2]. Other approaches jointly estimate the direct and reflected signal parameters [3].

In this paper, we address the positioning of a land vehicle in an urban environment by using nonlinear filtering techniques. Several previous works apply such filtering techniques to land vehicle positioning, Extended Kalman Filter (EKF) and Particle Filter being the filtering techniques commonly used [4, 5, 6].

Funding for this work was provided within the framework of the European project Eureka "EGNOS-BUS" No 3398.

Obtaining good estimates in the EKF framework requires a good knowledge on both dynamic process and measurement models, in addition to the assumption that both the process and measurement are corrupted by zero-mean white noises. The divergence due to modelling errors is a critical problem in Kalman filter applications. If the theoretical behavior of a filter and its actual behavior do not agree, divergence may occur. In Kalman filtering, the system model, system initial conditions, and noise characteristics have to be specified a priori. In various circumstances, there are uncertainties in the system model and noise description, and the assumptions on the statistics of disturbances are violated [7]. To prevent divergence problems due to modelling errors using the EKF approach, the adaptive filter algorithm has been one of the strategies considered for estimating the state vector [4, 8]. On the other hand performance degradation occurs when the actual noises are not Gaussian. In this case, the use of Gaussian Sum filtering approach is required [9]. In such approach, instead of using a single EKF, several EKFs are considered in parallel.

In this paper, we model the land vehicle positioning as a nonlinear and non-Gaussian problem. So, we make use of a Gaussian Sum Filter (GSF). We also point out a relation between the carrier-to-noise ratio (C/No) and multipaths. We derive a kind of adaptive GSF controlled by the C/No. Note that, due to economical issues, a major constraint of this work was to carry out a device that does not significantly increase the price of a standard GPS receiver. As a consequence, in addition to the GPS receiver, we make use of only one sensor, the odometer. Moreover, contrary to what is usually done (see [6, 10] for example), we make use of pseudo-ranges instead of positions delivered by the GPS receiver.

2. SYSTEM MODELS

In this section, we denote by ϵ^x a zero-mean Gaussian noise associated with the process x.

2.1. Vehicle motion model

Let us consider a vehicle located at each time t by the triple (x_t, y_t, z_t) given as ENU (East-North-Up) coordinates. Its motion in the horizontal plan can be described as follows:

$$x_t = x_{t-1} + \cos(\theta_{t-1}) v_{t-1} \Delta T \tag{1}$$

$$y_t = y_{t-1} + \sin(\theta_{t-1}) v_{t-1} \Delta T \tag{2}$$

where, θ_t et v_t denote respectively the vehicle heading and speed, ΔT being the sampling period. Notice that the vehicle motion in the horizontal plan is controlled by the driver. However, on the vertical plan, the vehicle undergoes the altitude variations inherent to the geographical area. These variations are slopes which can be viewed as random. Then a random walk can be sufficient for modelling such a motion. The vehicle speed can also be modelled in the same way:

$$z_t = z_{t-1} + \epsilon_t^z. \tag{3}$$

$$v_t = v_{t-1} + \epsilon_t^v. \tag{4}$$

Usually, the heading variations are modelled using steering angle [6], which is observed by means of a steering sensor. Such a sensor being out of the specifications of this work, we model heading variations by means of jumping processes:

$$\theta_t = \theta_{t-1} + \epsilon_t^\theta + a_t^\theta \Delta N_t^\theta, \tag{5}$$

a_t^θ being an uniform white noise on $[-\theta_{max}, \theta_{max}]$ representing a new heading and ΔN_t^θ a Poisson jump with frequency β corresponding to the frequency of heading change. Indeed, in an urban environment, one can consider that the vehicle trajectory is constituted with straight lines. Its heading can be viewed as nearly constant by portion of trajectory.

2.2. Sensor models

The vehicle motion is measured through two sensors: an odometer and a GPS receiver. The later can be configured to receive at the same frequency the odometer pulses and the pseudo-range measurements. For a given measurement period ΔT, the number n_t of the odometer pulses are related to the vehicle speed as follows:

$$n_t = \frac{\Delta T}{g_t} v_t + \epsilon_t^n \tag{6}$$

ϵ_t^n being the observation noise modelled as white Gaussian and g_t a possibly unknown scale factor modelled as:

$$g_t = g_{t-1} + \epsilon_t^g. \tag{7}$$

The pseudo-range measurements once corrected from ionospheric and tropospheric delay and from satellite clock bias are given by:

$$\rho_t^k = \sqrt{(X_t^k - X_t)^2 + (Y_t^k - Y_t)^2 + (Z_t^k - Z_t)^2} + ch_t + e_t^k, \tag{8}$$

(X_t^k, Y_t^k, Z_t^k) being the ECEF satellite coordinates, c the light speed, h_t the receiver clock bias, and e_t^k the residual noise viewed as the sum of an observation noise and a possible bias due to the multipath phenomenon.

By denoting d_t the clock drift, a second order model is used for describing the clock behavior:

$$h_t = h_{t-1} + d_{t-1}\Delta T + \Delta T \epsilon_t^h, \tag{9}$$

$$d_t = d_{t-1} + \Delta T \epsilon_t^d. \tag{10}$$

In order to take the presence of multipath bias into account, the residual noise e_t^k can be viewed as a white Gaussian noise with a time varying variance. Notice that multipaths appearance and disappearance can induce a variation of the power of the received signal. The quality of this signal is in particular given by the measurement of the C/No ratio. Hence, a link can be established between this measure and the variance of the residual noise. We suggest representing e_t^k as a white Gaussian noise with variance $\alpha 10^{-\frac{s_t^k}{10}}$, with s_t^k the C/No ratio and α a tuning parameter, or equivalently, as $e_t^k = 10^{-\frac{s_t^k}{20}} \epsilon_t^k$, with ϵ_t^k a white Gaussian noise with variance α.

2.3. State model

In ECEF (Earth Centred Earth Fixed) coordinates, the vehicle motion can equivalently be modelled as

$$\begin{pmatrix} X_t \\ Y_t \\ Z_t \end{pmatrix} = \begin{pmatrix} X_{t-1} \\ Y_{t-1} \\ Z_{t-1} \end{pmatrix} + \mathbf{A} \begin{pmatrix} \cos(\theta_{t-1}) v_{t-1} \Delta T \\ \sin(\theta_{t-1}) v_{t-1} \Delta T \\ \epsilon_t^z \end{pmatrix} \tag{11}$$

where $\mathbf{A}$, the matrix allowing conversion of coordinates from ENU (x_t, y_t, z_t) to ECEF (X_t, Y_t, Z_t), is given by:

$$\mathbf{A} = \begin{pmatrix} -\sin(\lambda) & -\sin(\phi)\cos(\lambda) & \cos(\phi)\cos(\lambda) \\ \cos(\lambda) & -\sin(\phi)\sin(\lambda) & \cos(\phi)\sin(\lambda) \\ 0 & \cos(\phi) & \sin(\phi) \end{pmatrix}, \tag{12}$$

$$\phi = \arctan \frac{Z_r}{\sqrt{X_r^2 + Y_r^2}}, \lambda = \arctan \frac{Y_r}{X_r}. \tag{13}$$

(X_r, Y_r, Z_r) being the ECEF coordinates of a local reference point. By defining the state vector as: $\mathbf{x}_t = (X_t \ Y_t \ Z_t \ \theta_t \ v_t \ g_t \ d_t \ h_t)$, according to the values taken by the Poisson jump ΔN_t^θ two prediction models can be considered with the *a priori* probability π_j, with $j = 1, 2$ and $\pi_1 + \pi_2 = 1$:

$$\mathbf{x}_t = f(\mathbf{x}_{t-1}) + \mathbf{B}\mathbf{w}_t^j \tag{14}$$

with:

$$f(\mathbf{x}_{t-1}) = \begin{pmatrix} X_{t-1} + g_X(\theta_{t-1}) v_{t-1} \Delta T \\ Y_{t-1} + g_Y(\theta_{t-1}) v_{t-1} \Delta T \\ Z_{t-1} + g_Z(\theta_{t-1}) v_{t-1} \Delta T \\ \theta_{t-1} \\ v_{t-1} \\ g_{t-1} \\ d_{t-1} \\ h_{t-1} + d_{t-1}\Delta T \end{pmatrix}$$

$$\begin{aligned} g_X(\theta_{t-1}) &= -\sin(\lambda)\cos(\theta_{t-1}) - \sin(\phi)\cos(\lambda)\sin(\theta_{t-1}) \\ g_Y(\theta_{t-1}) &= \cos(\lambda)\cos(\theta_{t-1}) + \sin(\phi)\sin(\lambda)\sin(\theta_{t-1}) \\ g_Z(\theta_{t-1}) &= \cos(\phi)\sin(\theta_{t-1}) v_{t-1} \Delta T \end{aligned}$$

$$\mathbf{B} = \begin{pmatrix} \mathbf{b}(\phi, \lambda) & 0 & 0 \\ 0 & \mathbf{I}_3 & 0 \\ 0 & 0 & \mathbf{I}_2 \Delta T \end{pmatrix}, \quad \mathbf{b}(\phi, \lambda) = \begin{pmatrix} \cos(\phi)\cos(\lambda) \\ \cos(\phi)\sin(\lambda) \\ \sin(\phi) \end{pmatrix}$$

$$\mathbf{w}_t^j = \begin{pmatrix} \epsilon_t^z & \epsilon_t^{\theta, j} & \epsilon_t^v & \epsilon_t^g & \epsilon_t^d & \epsilon_t^h \end{pmatrix}^T.$$

Notice that all the noises ϵ_t^z, $\epsilon_t^{\theta,1}$, $\epsilon_t^{\theta,2}$, ϵ_t^v, ϵ_t^d, ϵ_t^h, and ϵ_t^g are white Gaussian with zero mean with the respective variances σ_z^2, σ_θ^2, $\sigma_\theta^2 + \frac{\theta_{max}^2}{3}$, σ_v^2, σ_d^2, σ_h^2, and σ_g^2.

The observation model constructed from equations (6) and (8) is given by:

$$\mathbf{y}_t = m(\mathbf{x}_t) + \mathbf{C}_t \mathbf{z}_t, \tag{15}$$

where $\mathbf{y}_t = \begin{pmatrix} n_t & \rho_t^1 & \rho_t^2 & \cdots & \rho_t^K \end{pmatrix}^T$, K being the number of observed satellites,

$$m(\mathbf{x}_t) = \begin{pmatrix} \frac{\Delta T}{g_t} v_t \\ \sqrt{(X_t^1 - X_t)^2 + (Y_t^1 - Y_t)^2 + (Z_t^1 - Z_t)^2} + ch_t \\ \vdots \\ \sqrt{(X_t^K - X_t)^2 + (Y_t^K - Y_t)^2 + (Z_t^K - Z_t)^2} + ch_t \end{pmatrix},$$

$$\mathbf{z}_t = \begin{pmatrix} \epsilon_t^n \ \epsilon_t^1 \ \cdots \ \epsilon_t^K \end{pmatrix}^T, \ \mathbf{C}_t = \mathrm{diag}\left(1, \ 10^{-\frac{s_t^1}{20}}, \ \cdots, \ 10^{-\frac{s_t^K}{20}}\right).$$

In summary the system state model is as follows:

$$\begin{cases} \mathbf{x}_t = f(\mathbf{x}_{t-1}) + \mathbf{B}\mathbf{w}_t \\ \mathbf{y}_t = m(\mathbf{x}_t) + \mathbf{C}_t \mathbf{z}_t \end{cases} \tag{16}$$

where

$$\mathbf{w}_t \sim \pi_1 \Gamma(\mathbf{w}_t, \mathbf{Q}_1) + \pi_2 \Gamma(\mathbf{w}_t, \mathbf{Q}_2), \tag{17}$$

$$\mathbf{z}_t \sim \Gamma(\mathbf{z}_t, \mathbf{R}), \tag{18}$$

$\Gamma(\mathbf{a}, \mathbf{C})$, $\mathbf{a} \in \Re^{N\times 1}$, $\mathbf{C} \in \Re^{N\times N}$, denoting a multivariate Gaussian distribution with zero mean and covariance matrix $\mathbf{C}$. The covariance matrices are given by:

$$\begin{aligned} \mathbf{Q}_1 &= \mathrm{diag}\left(\sigma_z^2, \sigma_\theta^2, \sigma_v^2, \sigma_g^2, \sigma_d^2, \sigma_h^2\right) \\ \mathbf{Q}_2 &= \mathrm{diag}(\left(\sigma_z^2, (\sigma_\theta^2 + \theta_{max}^2/3), \sigma_v^2, \sigma_g^2, \sigma_d^2, \sigma_h^2\right) \\ \mathbf{R} &= \mathrm{diag}\left(\sigma_n^2, \alpha, \alpha, \cdots, \alpha\right) \end{aligned}$$

where $\mathrm{diag}(.)$ denotes the operator that forms a diagonal matrix with the vector in argument. Recall that K denotes the number of observed satellites, which is time varying.

3. GAUSSIAN SUM FILTERS

The sum of Gaussian structure is a general structure for filtering nonlinear systems in non-Gaussian disturbances and noise [9]. As described in (17), the process noise is given by a mixture of two Gaussians. According to (16), we get:

$$p(\mathbf{x}_t|\mathbf{x}_{t-1}) = \sum_{j=1}^{2} \pi_j \Gamma(\mathbf{x}_t - f(\mathbf{x}_{t-1}), \mathbf{B}\mathbf{Q}_j\mathbf{B}^T)$$

and $p(\mathbf{y}_t|\mathbf{x}_t) = \Gamma(\mathbf{y}_t - m(\mathbf{x}_t), \mathbf{R}_t)$. At time zero, our prior knowledge about $\mathbf{x}_0$ is summarized by $p(\mathbf{x}_0) = \sum_{n=1}^{N} \mu_0^n \Gamma(\mathbf{x}_0 - \bar{\mathbf{x}}_0^n, \mathbf{P}_0^n)$, with $\sum_{n=1}^{N} \mu_0^n = 1$. Assuming that, at time $t-1$, the prior distribution can be expressed as

$$p(\mathbf{x}_{t-1}|\mathbf{y}_{1:t-1}) = \sum_{n=1}^{N} \mu_{t-1}^n \Gamma(\mathbf{x}_{t-1} - \mathbf{x}_{t-1|t-1}^n, \mathbf{P}_{t-1|t-1}^n),$$

with $\sum_{n=1}^{N} \mu_{t-1}^n = 1$, we get:

$$\begin{aligned} p(\mathbf{x}_t|\mathbf{y}_{1:t-1}) &= \int_{\Re^8} p(\mathbf{x}_t|\mathbf{x}_{t-1}) p(\mathbf{x}_{t-1}|\mathbf{y}_{1:t-1}) d\mathbf{x}_{t-1} \\ &= \sum_{j=1}^{2}\sum_{n=1}^{N} \pi_j \mu_{t-1}^n \Gamma(\mathbf{x}_t - \mathbf{x}_{t|t-1}^n, \mathbf{P}_{t|t-1}^{n,j}), \end{aligned}$$

with:

$$\mathbf{x}_{t|t-1}^n = f(\mathbf{x}_{t-1|t-1}^n) \tag{19}$$

$$\mathbf{P}_{t|t-1}^{n,j} = \mathbf{F}(\mathbf{x}_{t-1|t-1}^n)\mathbf{P}_{t-1|t-1}^n \mathbf{F}(\mathbf{x}_{t-1|t-1}^n)^T + \mathbf{B}\mathbf{Q}_j\mathbf{B}^T \tag{20}$$

$\mathbf{F}(\mathbf{x}_{t-1|t-1}^n)$ being the Jacobian of $f(.)$ evaluated at $\mathbf{x}_{t-1|t-1}^n$. After the arrival of $\mathbf{y}_t$, the posterior distribution can be expressed as

$$p(\mathbf{x}_t|\mathbf{y}_{1:t}) = \frac{p(\mathbf{y}_t|\mathbf{x}_t)p(\mathbf{x}_t|\mathbf{y}_{1:t-1})}{\int_{\Re^8} p(\mathbf{y}_t|\mathbf{x}_t)p(\mathbf{x}_t|\mathbf{y}_{1:t-1})d\mathbf{x}_t}$$

$$\propto \sum_{j=1}^{2}\sum_{n=1}^{N} \pi_j \mu_{t-1}^n \Gamma(\mathbf{y}_t - m(\mathbf{x}_{t|t-1}^n), \mathbf{S}^{n,j})\Gamma(\mathbf{x}_t - \mathbf{x}_{t|t}^{n,j}, \mathbf{P}_{t|t}^{n,j})$$

with:

$$\mathbf{S}^{n,j} = \mathbf{M}(\mathbf{x}_{t|t-1}^n)\mathbf{P}_{t|t-1}^{n,j}\mathbf{M}(\mathbf{x}_{t|t-1}^n)^T + \mathbf{C}_t\mathbf{R}\mathbf{C}_t^T \tag{21}$$

$$\mathbf{K}^{n,j} = \mathbf{M}(\mathbf{x}_{t|t-1}^n)\mathbf{P}_{t|t-1}^{n,j}\left(\mathbf{S}^{n,j}\right)^{-1} \tag{22}$$

$$\mathbf{x}_{t|t}^{n,j} = \mathbf{x}_{t|t-1}^n + \mathbf{K}_t^{n,j}\left(\mathbf{y}_t - m(\mathbf{x}_{t|t-1}^n)\right) \tag{23}$$

$$\mathbf{P}_{t|t}^{n,j} = \mathbf{P}_{t|t-1}^{n,j} - \mathbf{K}^{n,j}\mathbf{M}(\mathbf{x}_{t|t-1}^n)\mathbf{P}_{t|t-1}^{n,j} \tag{24}$$

$\mathbf{M}(\mathbf{x}_{t|t-1}^n)$ being the Jacobian matrix associated with $m(.)$ and evaluated at $\mathbf{x}_{t|t-1}^n$. Then, after normalization, the posterior distribution is given by $p(\mathbf{x}_t|\mathbf{y}_{1:t}) \simeq \sum_{j=1}^{2}\sum_{n=1}^{N} \mu_t^{n,j}\Gamma(\mathbf{x}_t - \mathbf{x}_{t|t}^{n,j}, \mathbf{P}_{t|t}^{n,j})$, with $\mu_t^{n,j} = \frac{\pi_j \mu_{t-1}^n \Gamma(\mathbf{y}_t - m(\mathbf{x}_{t|t-1}^n), \mathbf{S}^{n,j})}{\sum_{i=1}^{2}\sum_{n=1}^{N} \mu_{t-1}^n \Gamma(\mathbf{y}_t - m(\mathbf{x}_{t|t-1}^n), \mathbf{S}^{n,i})}$. One can note that the number of mixands grows exponentially with the arrival of new observations. In practice, in order to limit the increase in the number of these mixands, a stage of selection can be necessary. Thus, for keeping this number equals to N, at each time, the Gaussians having the greatest weights should be selected, before an additional normalization step.

4. GPS POSITIONING EXPERIMENTS

In this section we describe our experimental results. Tests have been carried out in a district of Toulouse (France). The experimental field included an area of good visibility with no building or other big object in the vicinity and comprising a very broad avenue, a second area bordered of tall trees and buildings and comprising narrow streets, and a third area having broader streets but high buildings in the neighborhoods and some trees. Multipaths occur mainly in the two last areas. The collected data set is a very rich data set that has information with different GPS cover scenarios.

The vehicle was equipped with a μblox TIM-LR GPS receiver, a GPS Trimble 39265-50 3V polarized RHCP antenna, an odometer connected to the GPS receiver, and a computer for data saving. The measurement frequency was set to 4 Hz. Raw data were post-processed using the EUROCONTROL PEGASUS software for applying ionospheric, tropospheric, and satellite clock corrections.

The following settings were considered for the GSFs:

- $\pi_1 = 0.95$, $\pi_2 = 0.05$, $\theta_{max} = \pi/8$, $\sigma_\theta = \theta_{max} \times 10^{-7}$, $\sigma_z = 0.01m$, $\sigma_v = 1m/s$, $\sigma_d = 10^{-4}$, $\sigma_h = 10^{-4}$, $\sigma_g = 10^{-5}$, $\sigma_n = 1$, $N = 20$, $\Delta T = 0.25s$.

We first evaluate the effect of the observation noise covariance matrix modelling. We denote by GSF-FV(γ), the GSF with fixed values of the observation noise variance, i.e. $\mathbf{C}_t = \mathbf{I}_{K+1}$ and $\mathbf{R} = \mathrm{diag}\left(\sigma_n^2, \gamma, \cdots, \gamma\right)$. We compare GSF-FV($\gamma$) for different values of γ with GSF in Figure 1.

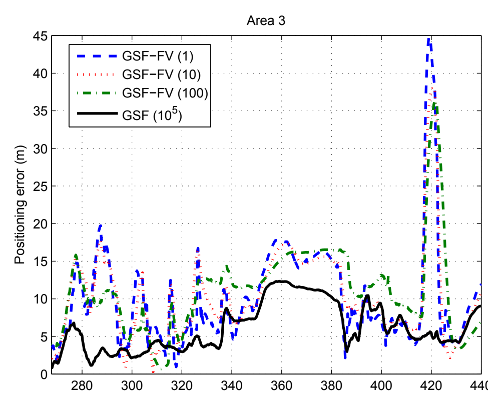

Fig. 1. Comparison of the positioning error between GSF-FV (γ) and GSF

For GSF, α was set equal to $\alpha = 10^5$. One can note that in general GSF-FV(γ), due to a fixed value of the observation noise covariance matrix, gives worst results than GSF with the proposed modelling. GSF allows avoiding or at least reducing some positioning error jumps.

Now, we evaluate the GSF algorithm by considering different values of α. Figure 2 depicts the positioning error obtained when using GSF for different values of α. One can note that no value of α guarantees the best performance at each time.

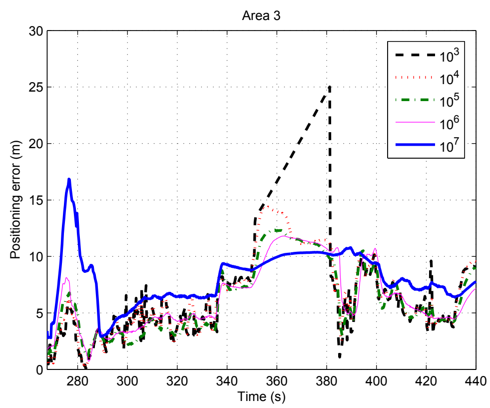

Fig. 2. GSF Positioning error according to α.

However, if one is interested with the mean performances, one can note that $\alpha = 10^5$ and $\alpha = 10^6$ give the best results (see Fig 3).

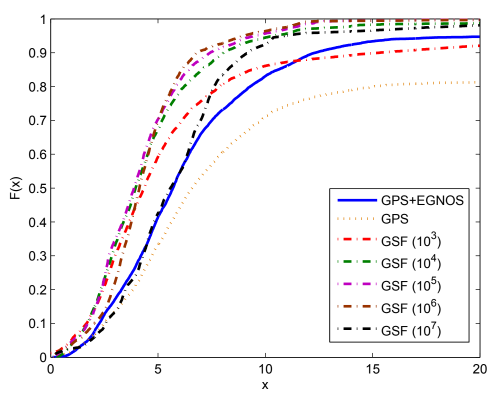

Fig. 3. Cumulative Distribution Function of the positioning error.

We also note that GSF outperforms standard GPS solution and GPS coupled with EGNOS solution. In Figure 4, we can see that GSF allows avoiding or reducing some jumps.

5. CONCLUSION

In this paper we have presented a land vehicle positioning method based on GPS pseudo-range and odometer measurements. The proposed method makes use of the carrier-to-noise ratio in order to control the covariance matrix associated with the observation noise. Such an approach allows mitigating multipaths errors. The proposed method was evaluated by the experimentation of a land vehicle in an urban environment. The results showed that the positioning accuracy is significantly improved compared to conventional GPS solutions.

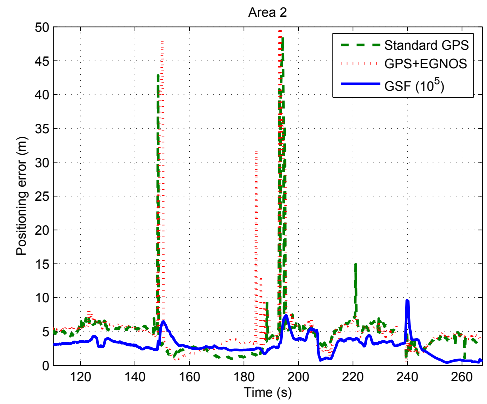

Fig. 4. Comparison of GSF with standard algorithms.

Acknowledgements: The authors would like to thank NAVOCAP S.A. for collecting the experimental data.

6. REFERENCES

[1] M. Antonini, M. Ruggieri, R. Prasad, U. Guida, and G.F. Corini, "Vehicular remote tolling services using EGNOS," *IEEE Aerospace and Electronic Systems Magazine*, vol. 20, no. 10, pp. 3–8, 2005.

[2] L. Garin and J. Rousseau, "Enhanced strobe correlator multipath rejection for code and carrier," in *Proc. ION GPS-97*, Kansas City, MO, September 16-19 1997.

[3] R.A. Iltis, "Joint estimation of PN code delay and multipath using the extended Kalman filter," *IEEE Trans. Communications*, vol. 38, no. 10, pp. 1677–1685, 1990.

[4] C. Hu, W. Chen, Y. Chen, and D. Liu, "Adaptive Kalman filtering for vehicle navigation," *Journal of Global Positioning Systems*, vol. 2, no. 1, pp. 42–47, 2003.

[5] D. Bevly and B. Parkinson, "Cascaded Kalman filters for accurate estimation of multiple biases, dead-reckoning navigation, and full state feedback control of ground vehicles," *IEEE Trans. on Control Systems Technology*, vol. 15, no. 2, pp. 199–208, 2007.

[6] F. Caron, M. Davy, E. Duflos, and P. Vanheeghe, "Particle filtering for multisensor data fusion with switching observation models: Application to land vehicle positioning," *IEEE Trans. on Signal Processing*, vol. 55, no. 6, pp. 2703–2719, 2007.

[7] D.-J. Jwo and S.-H. Wang, "Adaptive fuzzy strong tracking extended Kalman filtering for GPS navigation," *IEEE Sensors Journal*, vol. 7, no. 5, pp. 778–789, 2007.

[8] A. H. Mohamed and K.P. Schwarz, "Adaptive Kalman filtering for INS/GPS," *Journal of Geodesy*, vol. 73, no. 4, pp. 193–203, 1999.

[9] D.L. Alspach and H.W. Sorenson, "Nonlinear bayesian estimation using Gaussian sum approximations," *IEEE Trans. on Automatic Control*, vol. 17, no. 4, pp. 439–447, September 1972.

[10] R. Zickel and N. Nahemia, "GPS aided dead reckoning navigation," in *Navigating the earth and beyond; Proceedings of the 1994 National Technical Meeting*, San Diego, CA, Jan. 24-26 1994, pp. 577–586.